International Journal of Astrophysics and Space Science
2025; 13(3): 73-82
http://www.sciencepublishinggroup.com/j/ijass
doi: 10.11648/j.ijass.20251303.11
ISSN: 2376-7014 (Print); ISSN: 2376-7022 (Online)

A Concise Review on Exploring Dynamics of Equatorial Plasma Bubbles Within the Ionosphere

Amsalu Hundesa Dinede[1, 2, *]

[1]Department of Physics, Washera Geospace and Radar Science Research Laboratory, Bahir Dar, Ethiopia
[2]Department of Physics, College of Science, Bonga University, Bonga, Ethiopia

Email address:

amse2022amse2014@gmail.com (Amsalu Hundesa Dinede)
*Corresponding author

To cite this article:

Amsalu Hundesa Dinede. (2025). A Concise Review on Exploring Dynamics of Equatorial Plasma Bubbles Within the Ionosphere. *International Journal of Astrophysics and Space Science, 13*(3), 73-82. https://doi.org/10.11648/j.ijass.20251303.11

Received: 26 September 2024; **Accepted:** 16 December 2024; **Published:** 14 July 2025

Abstract: Equatorial Plasma Bubbles (EPBs) are complex and intriguing ionospheric phenomena characterized by localized regions of significantly depleted electron density, surrounded by areas of enhanced plasma density. These phenomena primarily occur after sunset and pose critical challenges to modern technologies reliant on ionospheric signal propagation, such as satellite navigation, radio communications, and space-based operations. The formation of EPBs is closely associated with the Rayleigh-Taylor instability (RTI), a plasma instability triggered by the interplay of gravitational forces and steep density gradients in the equatorial ionosphere. EPBs are initiated during the post-sunset period, driven by the pre-reversal enhancement (PRE) of the zonal electric field, which uplifts the ionospheric F-layer to altitudes where plasma density gradients intensify. This eastward electric field amplifies the RTI, expediting the growth of large-scale ionospheric depletions that evolve into the intricate structures characteristic of EPBs. The variability in the strength of the PRE and associated F-layer uplift significantly influences the initiation or inhibition of EPBs, resulting in complex spatial and temporal patterns of occurrence. Observational studies utilizing radar, ionograms, airglow imaging, and satellite measurements have provided a detailed understanding of EPB morphology and dynamics. These studies reveal that EPBs typically develop into elongated structures aligned with the Earth's magnetic field, exhibiting significant variability influenced by factors such as geomagnetic activity, seasonal changes, and atmospheric dynamics. EPBs are of profound scientific and practical significance due to their disruptive impact on radio wave propagation. They induce signal scintillation, degrade satellite-based navigation accuracy, and increase errors in communication systems. These effects make EPBs a critical area of study within space weather and ionospheric physics. This paper presents an expanded overview of the mechanisms underlying EPB formation, their evolution, and their impact on ionospheric processes and communication systems. By synthesizing theoretical and observational insights, this work aims to contribute to a deeper understanding of EPB dynamics and advance predictive capabilities for mitigating their effects on modern technologies.

Keywords: Equatorial Ionosphere, Equatorial Ionospheric Anomaly, Equatorial Plasma Bubbles, Rayleigh-Taylor Instability

1. Introduction

Equatorial plasma bubbles (EPBs) are interesting phenomena that occur in the ionosphere, particularly in the equatorial and low-latitude regions [1, 2]. They are characterized by regions of depleted electron density surrounded by areas of augment electron density. These irregularities in electron density can vary greatly in scale, from just a few meters to thousands of kilometers [3, 4]. EPBs are primarily observed after sunset when the ionosphere undergoes changes due to the transition from day to night [5, 6]. During the day, the ionosphere is primarily ionized by solar radiation, but as the sun sets, the ionization decreases, leading to the formation of these plasma bubbles. These bubbles can have significant impacts on radio communications, satellite navigation systems, and other technologies that rely on the ionosphere for signal propagation [7]. Equatorial ionospheric plasma depletions, also known as equatorial plasma bubbles, are slender east-west channels of rising

plasma triggered by instability in the lower F-region of the equatorial ionosphere. In this region, the gravitational force and density gradient act in opposite directions, causing the Rayleigh-Taylor instability (RTI) [8]. Various factors line up for the RTI to begin, particularly in connection with equatorial spread F. This instability is likely triggered by substantial upward vertical drifts and a prominent F-layer. Conversely, downward vertical and poleward meridional winds stabilize the F-region, slow down the formation of bubbles [9].The formation and evolution of these density depletion regions or plasma bubbles after sunset can give rise to highly intricate structures. EPBs have been investigated for several decades utilizing various methodologies, including radar observations [10], ionogram analysis [11, 12], airglow detection [13], and in-situ satellite measurements [14]. The Global Positioning by Satellite (GPS) network has also facilitated the study of these irregularities across large regions simultaneously, leveraging phase fluctuations at L1 and L2 frequencies [15] and correlating total electron content (TEC) depletions with scintillations [16]. Plasma irregularities and depletions associated with EPBs are typically observed during the nighttime, shortly after sunset, and sometimes persisting until a few hours after midnight [17, 18]. Previous studies have outlined the overall characteristics of EPBs, including their source mechanism, evolution processes, spatial structures, and global distributions, utilizing both ground and satellite-based observations. Analysis of these observations indicates that EPBs often originate in the post-sunset period due to the pre-reversal enhancement (PRE) in the zonal electric field, which abruptly lifts plasma to higher altitudes, creating a steep plasma density gradient in the bottomside F-layer. This sets the stage for the development of irregularities through the RTI in the bottom side ionosphere, followed by their transport to the topside ionosphere and higher latitudes along magnetic field lines. The eastward post-sunset electric field amplifies the RTI, while the westward electric field may suppress it [19, 20]. These instabilities can evolve into large-scale ionospheric depletions known as equatorial plasma bubbles. Equatorial Plasma Bubbles (EPBs) are large-scale ionospheric depletions that originate from the nonlinear evolution of the Rayleigh-Taylor instability (RTI) in the lower region of the equatorial F-layer [21]. This instability arises when regions of high-density plasma and magnetic flux tubes from the lower F-layer interchange with lower-density flux tubes from beneath. As the instability progresses, the depleted flux tubes ascend to higher altitudes, forming plasma bubbles.The pre-reversal enhancement (PRE) of the zonal electric field, which occurs after sunset, plays a pivotal role in influencing the F-layer uplift and modulating the conditions for EPB initiation or inhibition. Favorable conditions amplify RTI growth, enabling the development of these plasma depletions [10, 22].

EPBs significantly impact radio wave propagation, disrupt satellite communications [9], and degrade Global Navigation Satellite System (GNSS) signal accuracy. As a result, they remain a critical area of focus in space weather and ionospheric physics research. This paper aims to provide a concise review of the dynamics and development of EPBs, emphasizing their implications for technological systems and scientific understanding.

2. Growth Rates of the Rayleigh-Taylor Instability (RTI)

The current (J) due to gravitational gradient is given by

$$J_x = \frac{nMg}{B} = \frac{nMg \times B}{B^2} \tag{1}$$

The velocity of ion (V_i) due to electric and gravitational filed is given by:

$$V_i \perp = \frac{1}{1+k_i^2} w_i \perp + \frac{k_i}{1+k^2 i} wi \perp \times B \tag{2}$$

Where, $w_i = \frac{q}{M i v_{in}} E - Di \frac{\Delta n}{n} + \frac{\delta}{v_{in}}$. The system is unstable when g and ∇n are oppositely directed. The velocity of electron is given by

$$V_e = \frac{E \times B}{B} + \frac{kbTe}{enB^2}(\Delta E \times B) - \frac{meVen}{eB^2} g \times B \tag{3}$$

In the F-region, $k_i >> 1$, and the term $1 + k^2 i \approx k^2 i$, then the velocity of ion can be written in the from of

$$Vi \perp = \frac{1}{k^2 i} wi \perp + \frac{1}{ki} wi \times B \tag{4}$$

Inserting wi into the above equation and rearranging

$$V_i \perp = \frac{eE}{K^2 i m_i v_{in}} + \frac{g}{v_{in} k^2 i} - \frac{D_i}{k^2 i}(\frac{\Delta n}{n}) + \frac{E \times B}{B^2} + \tag{5}$$
$$M(\tfrac{g \times B}{eB^2}) - \tfrac{kbT_i}{enB^2}(\Delta E \times B)$$

From equation (3) $g \times B$ term can be zero because m_e is small, in the same way equation (5) 2nd and 3rd terms are small due to $k_i >> 1$, then $n_i = n_e = n$. The $E \times B$ terms are identical for ions and electrons, therefore no current flow, then the current is given by

$$J = ne(V_i - V_e) \tag{6}$$

Using this term for velocity and yields

$$J = \frac{ne^2}{k^2 i m v_i} E + \frac{ne}{\Omega} g \times B - \frac{Kb}{B^2}(T_i + T_e)(\Delta \times B) \tag{7}$$

Where, $\Omega = \frac{eB}{m}$. The ion continuity equation at the F-region during post sun set is given by

$$\frac{\partial n}{\partial t} + V.\Delta n + n(\Delta.V) = 0 \tag{8}$$

From equation 5 $E = 0$, k_i is large and $M > m$ Considering

the compressibility term and velocity of ion, we can have

$$\Delta.V = \Delta.\left\{\frac{M}{eB^2}(g \times B) - (\frac{k_b T_i}{enB^2})(\Delta \times B)\right\} \quad (9)$$

since g and B do not varying in the $g \times B$, the first term vanishes. Also $\Delta.(\Delta n \times B) = 0$ and $(\Delta n \times B).\Delta n = 0$. This equation shows plasma flow is incompressible. Now the continuity and divergence of the current are given by

$$\frac{\partial n}{\partial t} + V.\Delta n = 0 \quad (10)$$

$$\Delta.J = 0 \quad (11)$$

From equation 11 and equation 7 and replacing E by ΔE

$$\Delta.J = \Delta.\left\{\frac{ne^2 V_{in}}{M\Omega^2}\Delta E + \frac{ne}{\Omega}g \times B - \frac{k_b}{B^2}(T_i + T_e)(\Delta \times B)\right\} \quad (12)$$

But $\Delta.(\Delta \times B) = 0$

$$\Delta.J = \Delta.\left\{\frac{ne^2 v_{in}}{M\Omega^2 i}\Delta E + \frac{ne}{\Omega}g \times B\right\} = 0 \quad (13)$$

For the current is owing along x and z, the continuity equation becomes

$$\frac{\partial n}{\partial t} + V_x\frac{\partial n}{\partial x} + v_z\frac{\partial n}{\partial z} = 0 \quad (14)$$

Where $v_x = \frac{Mg}{eB} = \frac{Q}{e}$ and $v_z = \frac{\Delta E_x}{B}$
Now the linearized continuity equation becomes

$$\frac{\partial n}{\partial t} + \frac{Q}{e}\frac{\partial n}{\partial x} - \frac{1}{B}\frac{\partial \phi}{\partial x}\frac{\partial n}{\partial z} = 0 \quad (15)$$

After certain rearrangement

$$w_i = -\frac{g}{v_{in}}(\frac{1}{n_o})(\frac{\partial n_o}{\partial z}) \quad (16)$$

When $\frac{\partial n_o}{\partial z}$ is positive corresponding to the density gradient anti parallel to g, w_i is negative and $e^{iwt} = e^{iw_r t}e^{\gamma t}$, where γ is positive and thus yields a growing solution. The parameter γ is the growth rate of the instability and is given by $\gamma = \frac{g}{Lv_{in}}$ where, L is the gradient scale length.When γ is increase the instability is also increase. Gravity is not the only destabilizing influence in the equatorial ionosphere.The following can also affect the growthr ate Eastward electric field enhance RT-instability while the west ward quench it and the neutral wind are the other parametrizes. According to [23] the generalized growth rate can be given by

$$\gamma = \frac{\sum_P^F}{\sum_P^E + \sum_P^F}(Vp - U_n^p - \frac{gL}{U_{in}^{eff}})\frac{1}{Ln} - RT \quad (17)$$

where, gL is the downw arda ccelerarion due to gravity, $Vp = \frac{E \times B}{B^2}$ is the vertical component of plasma drift due to the zonal component of the electric field E at the magnetic equator, U^{p_n} is the vertical component of the neutral wind velocity perpendicular to B. $u^{eff_{in}}$ is the effective flux-tube integrated F-region ion neutral collision frequency weighted by the number density in the flux tube, Ln is the scale length of the vertical gradient of the flux-tube integrated plasma density measured at the equator, RT is the flux-tube integrated recombination rate.

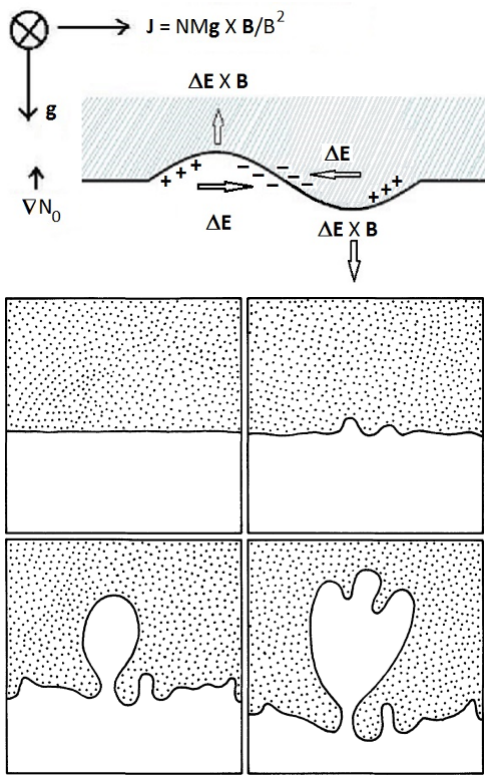

Figure 1. *Schematic diagram of the plasma analog of the Rayleigh-Taylor instability when the heavy uid is initially supported by a transparent lighter fluid geometry [24].*

The commonly accepted scenario for the formation of spread F and plasma bubbles is, during the day, the atmospheric wind generates a dynamo electric field in the lower ionosphere that is eastward, and this field is mapped to F-region altitudes along magnetic filed. The current $(\vec{J}_x)$ is along $g \times \vec{B}$ which is horizontal to the surface, and has divergence that pile up charges on the edges of the small initial perturbation, as a result perturbed electric filed (ΔE) is generated and force plasma to drift with $\Delta E \times B$ velocity. As we can observe from Figure (1), initial small oscillations in the surface grow "in place," pushing the lighter fluid upward. In the ionospheric case the "light fluid" is the low-density plasma, which carries a gravity-driven current that provides the $\vec{J} \times \vec{B}$ force, preventing the plasma from freely falling [21]. The eastward electric field, in combination with the northward magnetic field, produces an upward $\vec{E} \times \vec{B}$ drift of the F-region plasma [25].

As the ionosphere rotates with the Earth toward dusk, the eastward neutral wind strengthens, primarily blowing across the terminator from the dusk side to the dawn side. Plasma bubbles are more commonly formed in equatorial and low-latitude regions than in mid- and high-latitude areas. In these lower-latitude regions, ionospheric irregularities mainly affect the amplitude of plasma signals, with phase disturbances occurring less frequently. Post-sunset equatorial irregularities are mainly caused by the RTI. A study by [26] found that the strength of the electron density gradient between the crest and trough of the Equatorial Ionization Anomaly (EIA) is linked to the intensity of the electrodynamical vertical drift near sunset. This drift plays a crucial role in triggering equatorial spread-F (ESF) or plasma bubble irregularities. At low latitude regions the EIA is formed by combined effects of $\vec{E} \times \vec{B}$ drift and ambipolar diffusion [27].

2.1. Equatorial Ionization Anomaly (EIA)

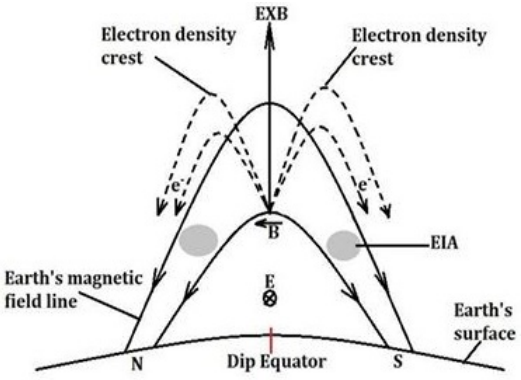

Figure 2. *A schematic diagram illustrating the equatorial fountain effect and upward plasma drift due to $E \times B$.*

The EIA is a distinctive feature of the Earth's ionosphere, observed near the geomagnetic equator [28]. It is characterized by an asymmetrical distribution of electron density between the northern and southern hemispheres, with the southern hemisphere often exhibiting higher ionization levels during the daytime. This asymmetry is most prominent during the equinoxes but varies throughout the day and across seasons.

The emergence and dynamics of the EIA result from a complex interplay of factors, including solar radiance, the Earth's geomagnetic architecture, and atmospheric neutral wind patterns [29]. During daylight hours, intense solar energy ionizes the upper atmosphere, leading to an abundance of free electrons. However, the geomagnetic equator the region where Earth's magnetic field is perfectly horizontal does not align with the geographic equator. Instead, it shifts toward the magnetic dip equator, introducing a latitudinal divergence between these reference points [30]. The displacement of the geomagnetic equator from the geographic equator plays a critical role in shaping the structure of the EIA. This misalignment, combined with solar driven ionization and geomagnetic influences, creates an imbalance in electron density distribution across low latitude regions. During the daytime, intense solar radiation ionizes the upper atmosphere, leading to a significant increase in free electrons. However, these charged particles do not remain uniformly distributed. Instead, they are influenced by the Earth's magnetic field and atmospheric dynamics, leading to distinct variations in electron density. One of the key mechanisms driving this asymmetry is the equatorial fountain effect, a phenomenon where ionospheric plasma is lifted vertically by the interaction of the equatorial electrojet and the Earth's magnetic field. This lifted plasma then moves along geomagnetic field lines, causing an outward and downward motion, ultimately leading to the formation of two bands of enhanced electron density on either side of the magnetic equator. These bands define the structure of the EIA and are a direct consequence of the latitudinal displacement between the geographic and geomagnetic equators . Additionally, atmospheric neutral winds play a crucial role in modulating the EIA. Thermospheric winds, influenced by solar heating, drive plasma transport along magnetic field lines, further contributing to the observed electron density variations. These winds can enhance or suppress the fountain effect depending on their direction and strength. During geomagnetic disturbances, electric fields and storm-induced changes in neutral winds can significantly alter the structure of the EIA, sometimes leading to the expansion or contraction of the anomaly regions [31]. The EIA is a highly dynamic and complex ionospheric phenomenon, influenced by a combination of solar activity, geomagnetic forces, and atmospheric interactions. Understanding its behavior is essential for studying ionospheric processes and predicting their impact on space weather and communication systems [32]. Since radio signals depend on the stability of the ionosphere, variations in electron density caused by the EIA can lead to signal delays, degradation, and even loss of communication in extreme cases. This makes the study of EIA crucial for improving satellite navigation, radio communication, and space weather forecasting [21]. This displacement of the geomagnetic equator also introduces a complex interplay of forces, where the equatorial ionosphere is subjected to the effects of the geomagnetic field. The Earth's magnetic field naturally pulls charged particles toward the magnetic poles, but in the equatorial region, the unique configuration of these forces results in a distinct plasma redistribution pattern. This redistribution is further modified by geomagnetic storms, which can enhance or suppress electron density variations depending on storm intensity and duration [33].

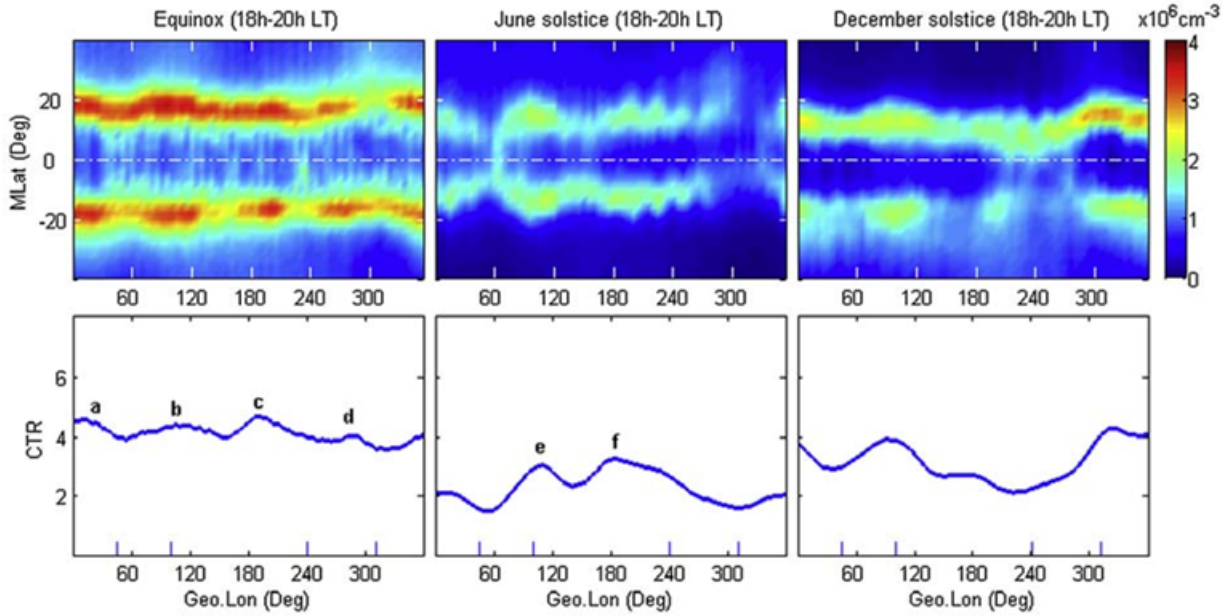

Figure 3. *Season/Longitude-dependent structures of evening EIA (18?20 h LT). (Top) Distribution of the electron density from CHAMP for quiet conditions at solar maximum. (Bottom) The CTR index derived from the electron density pro le (smooth curve of each panel is tted to the 15 longitudinal mean values) shown above [34].*

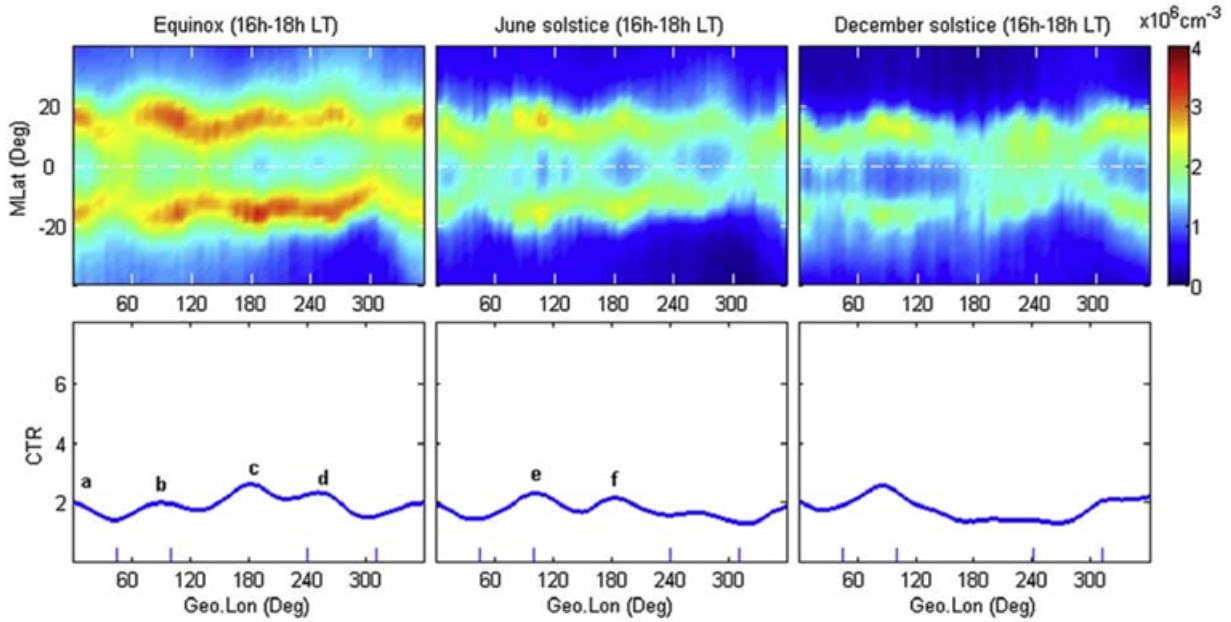

Figure 4. *Same as Figure 3 but for afternoon EIA (16-18 h LT). Figures 3 and 4 show that the seasonal distribution in the evening EIA is apparently stronger than that in the afternoon EIA for nearly all longitudes, but the wave-like small-scale variation in longitudinal distribution between them is similar, especially during equinox [34].*

Additionally, neutral winds in the upper atmosphere, driven by the complex interaction between the atmosphere and the underlying surface, can significantly influence the distribution of ionization. As a result of these interactions, the equatorial ionosphere exhibits a unique structure, characterized by a pronounced ionization crest in the southern hemisphere during the daytime hours. This crest gradually shifts towards the magnetic equator as evening approaches and disappears during the nighttime hours, leading to a more symmetrical ionization distribution between the hemispheres. The EIA has significant implications for radio wave propagation, satellite communications, and navigation systems operating in equatorial regions. Variations in electron density can affect the refraction and attenuation of radio signals, leading to signal degradation and communication disruptions.

At the geomagnetic equator, the magnetic field lines extend horizontally in a north-south direction [26]. Within the E-region ionosphere, tidal winds generate daytime currents,

leading to the accumulation of positive and negative charges at the dawn and dusk terminators, respectively. This creates a conductivity gradient, resulting in a pronounced eastward electric field along the magnetic equator. Consequently, the combined influence of the electric and magnetic fields drives electrons upward through electromagnetic drift $E \times B$ force. However, due to the constraint of the horizontal magnetic field lines, plasma diffuses along these lines due to pressure gradient and gravity. It settles approximately between $\pm 20^0$ degrees from the geomagnetic equator, contributing substantial electron masses to this region. The electron density data within period 18-20 h LT are sorted into longitude and latitude, the electron density peaks are located north and south of the magnetic equator, and the density trough is in between them. The 20^0 longitudinal mean values of EIA strength characterized by the crest to-trough ratio (CTR) index are presented in the above panels [26]. Figures 3 and 4 illustrate that the evening Equatorial Ionization Anomaly (EIA) tends to be more pronounced seasonally compared to the afternoon EIA across most longitudes. The significant correspondence observed between the large-scale longitudinal variation of the evening EIA and the prereversal $E \times B$ drifts, along with the intensified EIA strength around sunset, suggests a positive correlation between the prereversal enhancement and the EIA. These $E \times B$ drifts likely augment both the evening and afternoon EIA by stimulating the equatorial fountain effect and increasing plasma density at off-equatorial latitudes. Consequently, this leads to a substantial ionization anomaly during the post-sunset period, as evidenced by the higher CTR index depicted in Figure 3 compared to Figure 4. Consequently, this leads to a substantial ionization anomaly during the post-sunset period, as evidenced by the higher CTR index depicted in Figure 3 compared to Figure 4. The there are certain consistent small-scale variations observed in the longitudinal distribution of the evening EIA which correspond to the longitudinal variations seen in the afternoon EIA. This implies that the patterns observed in the distribution of ionization in the evening atmosphere mirror those seen in the afternoon, albeit on a smaller scale. Essentially, it suggests a continuity or similarity in the spatial distribution of ionization phenomena between the afternoon and evening periods, albeit with some variations.

2.2. Equatorial Plasma Bubbles

This study investigates the global distribution of the scintillation index (S4) to analyze the longitudinal characteristics of EPB occurrences. The analysis is based on observations at an altitude of 500 km, covering latitudes from $50°$S to $40°$N. Figure 5 illustrates the spatial distribution of EPBs, with a magenta line indicating the magnetic equator. The results show that scintillation events are primarily concentrated within $\pm 20°$ magnetic latitudes. However, the strength and frequency of these events exhibit a clear asymmetry around the magnetic equator. Specifically, the northern hemisphere experiences more intense scintillations than the southern hemisphere (Figure 5a).

Three major regions exhibit maximum S4 values, reaching 0.5. These regions are the Atlantic, Africa, and Asia. The occurrence of EPBs closely follows this pattern, as depicted in Figure 5b. The highest EPB occurrence rates, reaching up to 80%, are observed in these regions. In contrast, the Pacific region shows weaker EPB characteristics and lower occurrence frequencies. These findings align with previous studies on ionospheric irregularities in different longitudinal sectors [35].

Further analysis, presented in Figures 5 and 6, extends the investigation to the global distribution of S4 and sporadic E-layer (Es) events. The Es layer is observed at an altitude of 100 km, covering latitudes from $50°$ S to $40°$ N. This analysis reveals the longitudinal variability and regional dependencies of EPB and Es activity. Understanding these variations is crucial for improving ionospheric modeling and space weather forecasting.

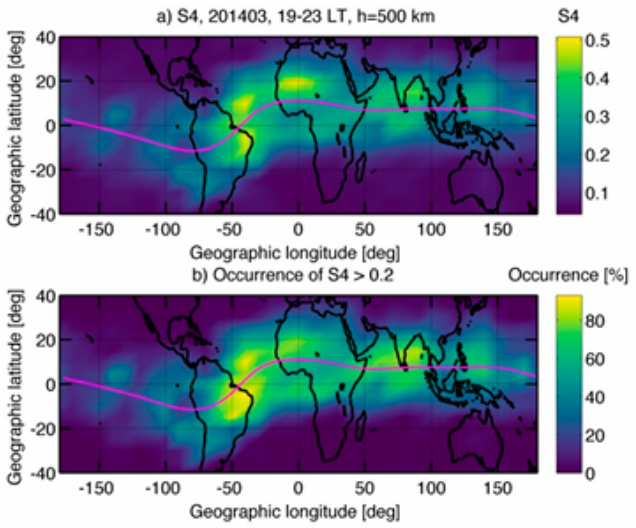

Figure 5. *Global distribution of (a) S4 and (b) the occurrence of S4 ¿ 02 at 500 km observed by COSMIC in March 2014 [36].*

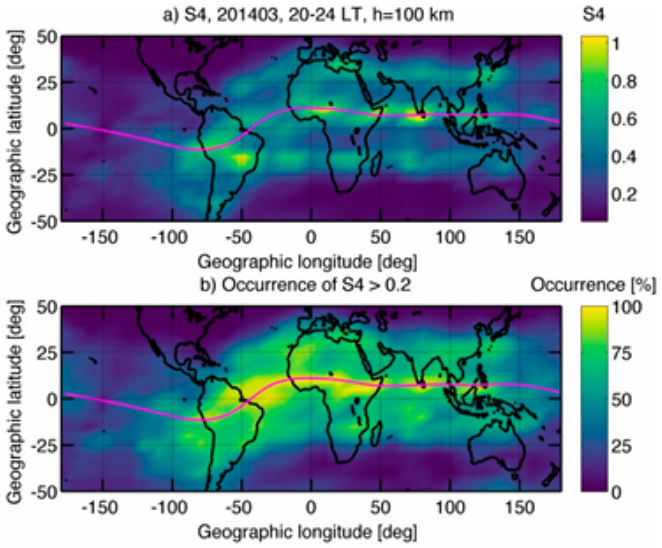

Figure 6. *Global distribution of (a) S4 and (b) the occurrence of S4 ¿ 02 at 100 km observed by COSMIC in March 2014 [36].*

2.3. Effect of Solar Activity on the Occurrences of EPBs

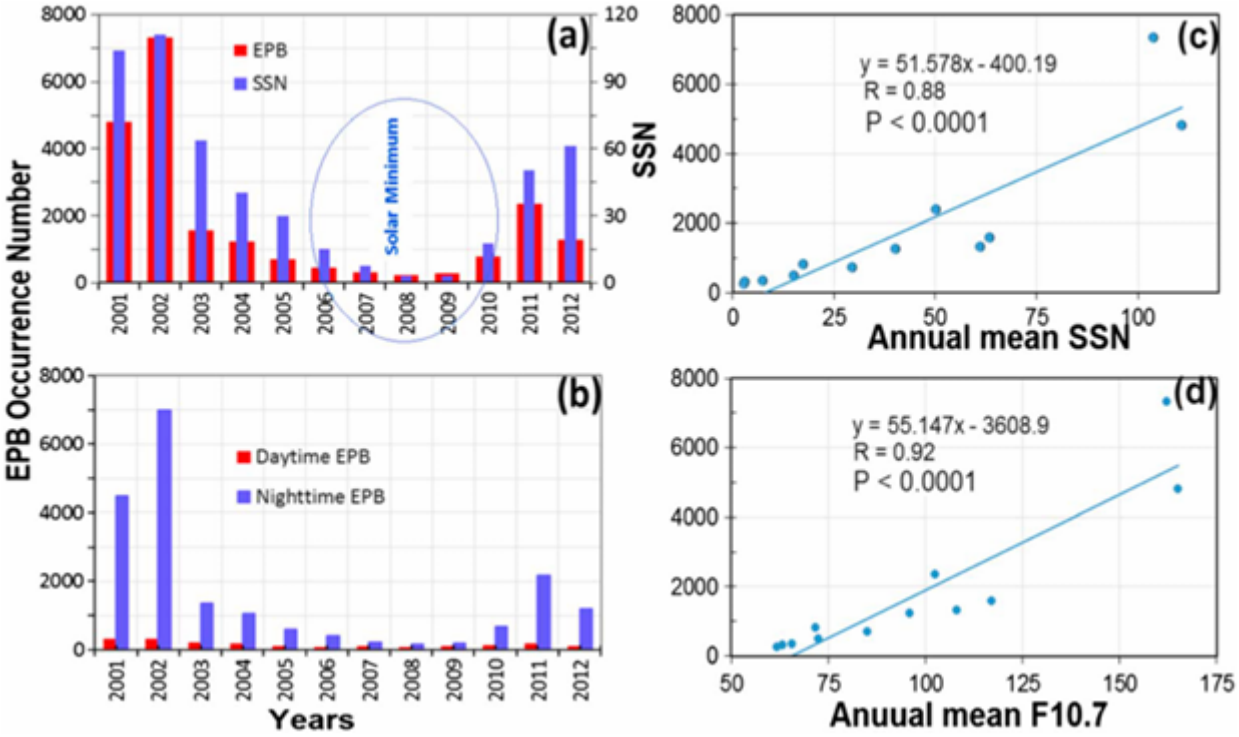

Figure 7. *(a) The study examined: (a) annual EPB occurrences from 2001 to 2012 alongside the yearly mean total sunspot number (SSN); (b) yearly daytime and nighttime EPB occurrences; (c) correlation scatter plot between annual total EPB occurrences and annual mean SSN; and (d) correlation scatterplot between annual total EPB occurrences and annual mean F10.7 cm solar flux. Correlation coefficients (R) and significance levels (P) for the datasets are provided [37].*

To explore the influence of solar activity on EPB occurrence, researchers examined the yearly count of EPBs during daytime, nighttime, and the total (day+night) alongside the sunspot number (SSN) from 2001 to 2012, as depicted in Figures 7a and 7b. Analysis of these figures reveals a clear correlation between EPB occurrence, both day and night, and SSN [38, 39]. Specifically, EPB occurrences peak during the solar maximum year of 2002 and hit a low point during the solar minimum year of 2008 [40, 43]. Further insight into this relationship is provided by Figures 7c and 7d, which present correlation analyses between total annual EPB occurrences and the annual mean SSN and F10.7 cm flux, respectively [37].

In periods of low solar activity, the yearly percentage of EPB occurrences was notably reduced, as depicted in Figure 8. Across all stations analyzed, there was a higher annual percentage of EPB occurrences during the peak solar activity years (2012-2014) and a lower percentage during periods of low solar activity (2008-2009). This correlation between annual EPB occurrence percentages and average annual SSN reaffirms findings previously documented by [3, 44, 45]. The positive correlation suggests that during high solar activity phases, there is an increase in solar Extreme Ultraviolet (EUV) radiation, which, upon reaching Earth, ionizes neutral particles in the upper atmosphere.

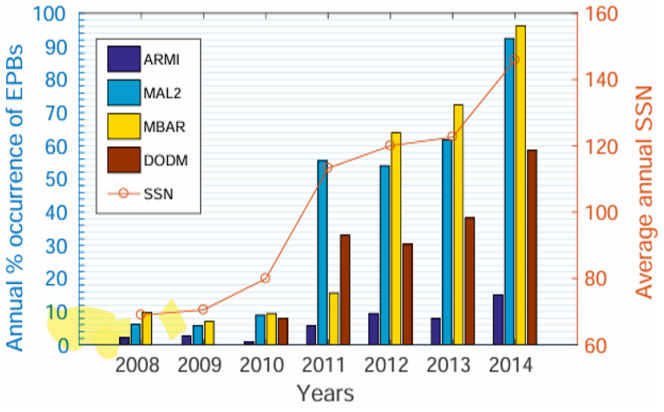

Figure 8. *The comparison involves the yearly percentage occurrence of EPBs across various locations and the average annual SSN [43].*

3. Conclusion

Equatorial Plasma Bubbles (EPBs) are intriguing ionospheric phenomena characterized by regions of depleted and enhanced electron densities. They primarily emerge after sunset due to the Rayleigh-Taylor instability, driven by gravitational forces and plasma density gradients. These bubbles significantly impact radio communications, satellite navigation, and other technologies reliant on stable ionospheric signal propagation. Their formation and evolution

are closely linked to the pre-reversal enhancement of the zonal electric field, underscoring their importance in space weather studies.

The Equatorial Ionization Anomaly (EIA) also plays a key role in EPB development by creating plasma density gradients along the magnetic equator, which amplify instabilities. Multiple factors contribute to the formation of EPBs, including the Rayleigh-Taylor instability, gravity waves, and plasma vertical drift. The interaction between EPBs and the EIA highlights the interconnected nature of these phenomena, making it essential to study them together for a deeper understanding of ionospheric dynamics.

In summary, gaining insights into EPBs is crucial for advancing ionospheric research and enhancing the resilience of technologies affected by space weather. Continued studies are necessary to develop predictive models and mitigation strategies, ultimately reducing the impact of EPBs on vital global systems like navigation and communication networks.

Acknowledgments

The authors gratefully acknowledge the Washera Geospace and Radar Science Research Laboratory in the Department of Physics at Bahir Dar University and Bonga University. Additionally, I extend my heartfelt gratitude to Prof. Tsegaye Kassa Gogie for his invaluable guidance and contributions to this work.

Ethics Approval

Ethics and Consent to Participate declarations not applicable.

Consent to Participate

Consent to Participate declaration not applicable.

Consent to Publish

Consent to Publish declaration not applicable.

Funding

The authors received no direct funding for this work.

Conflicts of Interest

The authors declare that they have no known competing financial interests or personal relationships that could have appeared to influence the work reported in this paper.

References

[1] Xiong, C., Stolle, C., Luhr, H., Park, J., Fejer, B. G., Kervalishvili, G. N. (2016) “Scale analysis of equatorial plasma irregularities derived from swarm constellation. Earth,” Planets and Space 68, 112. https://doi.org/ 10.1186/s40623-016-0502-5

[2] Patil, A. S., Nade, D. P., Taori, A., Pawar, R. P., Pawar, S. M., Nikte, S. S., Pawar, S. D.: A brief review of equatorial plasma bubbles. Space Science Reviews 219(1), 16 (2023). https://doi.org/10.1007/s11214-023-00958-y

[3] Gentile, L., Burke, W., Rich, F.: A global climatology for equatorial plasma bubbles in the topside ionosphere. In: Annales Geophysicae, vol. 24, pp. 163172 (2006). https://doi.org/10.5194/angeo-24-163-2006

[4] Katamzi-Joseph, Z. T., Habarulema, J. B., Hernandez-Pajares, M.: Midlatitude postsunset plasma bubbles observed over europe during intense storms in april 2000 and 2001. Space Weather 15(9), 1177 1190 (2017). https://doi.org/10.1002/2017SW001674

[5] Vankadara, R. K., Jamjareegulgarn, P., Seemala, G. K., Siddiqui, M. I. H., Panda, S. K.: Trailing equatorial plasma bubble occurrences at a low-latitude location through multi-gnss slant tec depletions during the strong geomagnetic storms in the ascending phase of the 25th solar cycle. Remote Sensing 15(20), 4944 (2023). https://doi.org/10.3390/rs15204944

[6] Edward, U., Boniface, N., George, O.: Occurrence characteristics of equatorial plasma bubbles over kisumu, kenya during solar maximum of solar cycle 24.

[7] Tsunoda, R. T.: Magnetic- eld-aligned characteristics of plasma bubbles in the nighttime equatorial ionosphere. Journal of Atmospheric and Terrestrial Physics 42(8), 743752 (1980). https://doi.org/10.1016/0021-9169(80)90057-4

[8] Carrasco, A. J., Pimenta, A. A., Wrasse, C. M., Batista, I. S., Takahashi, H.: Why do equatorial plasma bubbles bifurcate? Journal of Geophysical Research: Space Physics 125(11), 2020028609 (2020). https://doi.org/10.1029/2020JA028609

[9] Portillo, A., Herraiz, M., Radicella, S., Ciraolo, L.: Equatorial plasma bubbles studied using african slant total electron content observations. Journal of Atmospheric and Solar-Terrestrial Physics 70(6), 907917 (2008). https://doi.org/10.1016/j.jastp.2007.05.019

[10] Woodman, R. F., La Hoz, C.: Radar observations of f region equatorial irregularities. Journal of Geophysical.

[11] Whalen, J.: Equatorial bubbles observed at the north and south anomaly crests: Dependence on season, local time, and dip latitude. Radio Science 32(4), 15591566 (1997). https://doi.org/10.1029/97RS00285

[12] Hundesa, A.: Ionosonde data analysis for precise study of ionospheric electron density. Space Sci J 1(1), 0112 (2024). https://doi.org/10.21203/rs.3.rs-3990475/v1

[13] Mendillo, M., Baumgardner, J.: Airglow characteristics of equatorial plasma depletions. Journal of Geophysical Research: Space Physics 87(A9), 76417652 (1982). https://doi.org/10.1029/ja087ia09p07641

[14] Huang, C., Burke, W., Machuzak, J., Gentile, L., Sultan, P.: Dmsp observations of equatorial plasma bubbles in the topside ionosphere near solar maximum. Journal of Geophysical Research: Space Physics 106(A5), 81318142 (2001). https://doi.org/10.1029/2000JA000319

[15] Pi, X., Mannucci, A., Lindqwister, U., Ho, C.: Monitoring of global ionospheric irregularities using the worldwide gps network. Geophysical Research Letters 24(18), 22832286 (1997). https://doi.org/10.1029/97GL02273

[16] Gwal, A., Wahi, R., Dubey, S.: Simultaneous observation of scintillation and tec using gps receiver at low latitude station bhopal. In: Ionospheric E ects Symposium, pp. 607617 (2005).

[17] Ott, E.: Theory of rayleigh-taylor bubbles in the equatorial ionosphere. Journal of Geophysical Research: Space Physics 83(A5), 20662070 (1978). https://doi.org/10.1029/JA083iA05p02066

[18] Nyongesa, E., Ndinya, B., Omondi, G.: Occurrence characteristics of equatorial plasma bubbles over kisumu, kenya during solar maximum of solar cycle 24 (2021).

[19] Kelley, M. C., Kotsikopoulos, D., Beach, T., Hysell, D., Musman, S.: Simultaneous global positioning system and radar observations of equatorial spread f at kwajalein. Journal of Geophysical Research: Space Physics 101(A2), 23332341 (1996). https://doi.org/10.1029/95JA02025

[20] Garcia, F., Kelley, M., Makela, J., Huang, C.-S.: Airglow observations of mesoscale low-velocity traveling ionospheric disturbances at midlatitudes. Journal of Geophysical Research: Space Physics 105(A8), 18407 18415 (2000). https://doi.org/10.1029/1999JA000305

[21] Kelley, M. C.: The Earth s Ionosphere: Plasma Physics and Electrodynamics. Academic press, (2009).

[22] Scannapieco, A. J., Ossakow, S. L.: Nonlinear equatorial spread f. Geophysical Research Letters 3(8), 451454 (1976). https://doi.org/10.1029/GL003i008p00451

[23] Sultan, P.: Linear theory and modeling of the rayleigh-taylor instability leading to the occurrence of equatorial spread f. Journal of Geophysical Research: Space Physics 101(A12), 2687526891 (1996). https://doi.org/10.1029/96ja00682

[24] Bhattacharyya, A.: Equatorial plasma bubbles: A review. Atmosphere 13(10), 1637 (2022). https://doi.org/1410.3390/atmos13101637

[25] Schunk, R., Nagy, A.: Ionospheres: Physics, Plasma Physics, and Chemistry. Cambridge university press, (2009).

[26] Mendillo, M., Meriwether, J., Biondi, M.: Testing the thermospheric neutral wind suppression mechanism for day-to-day variability of equatorial spread f. Journal of Geophysical Research: Space Physics 106(A3), 36553663 (2001). https://doi.org/10.1029/2000JA000148

[27] Giday, N. M., Katamzi-Joseph, Z. T., Stoneback, R.: E ect of moderate geomagnetic storms on equatorial plasma bubbles over eastern africa in the year 2012: Evolution and electrodynamics. Advances in Space Research 65(7), 17011713 (2020). https://doi.org/10.1016/j.asr.2020.01.013

[28] De Rezende, L., De Paula, E., Kantor, I. J., Kintner, P.: Mapping and survey of plasma bubbles over brazilian territory. The Journal of Navigation 60(1), 6981 (2007). https://doi.org/10.1017/S0373463307004006

[29] Bharti, G., Bag, T., Krishna, M. S.: E ect of geomagnetic storm conditions on the equatorial ionization anomaly and equatorial temperature anomaly. Journal of Atmospheric and Solar-Terrestrial Physics 168, 820 (2018).

[30] Lech, B.: Evaluating the capability of icon-mighti to detect plasma bubbles in the ionosphere. PhD thesis, Virginia Tech (2024).

[31] Abdu, M. A.: Equatorial ionosphere thermosphere system: Electrodynamics and irregularities. Advances in Space Research 35(5), 771787 (2005).

[32] Rishbeth, H., Mendillo, M.: Patterns of f2-layer variability. Journal of Atmospheric and Solar-Terrestrial Physics 63(15), 16611680 (2001).

[33] Tsurutani, B., Mannucci, A., Ijima, B., Saito, A., Yumoto, K., Abdu, M., Gonzalez, W., Guarnieri, F., Tsuda, T., Fejer, B., et al.: Global dayside ionospheric uplift andenhancements due to interplanetary shock electric elds. Journal of Geophysical Research 109(A08302) (2004).

[34] Li, G., Ning, B., Liu, L., Zhao, B., Yue, X., Su, S.-Y., Venkatraman, S.: Correlative study of plasma bubbles, evening equatorial ionization anomaly, and equatorial prereversal e b drifts at solar maximum. Radio Science 43(04), 111 (2008). https://doi.org/10.1029/2007RS003760

[35] Shiokawa, K., Otsuka, Y., Ogawa, T., Wilkinson, P.: Time evolution of high-altitude plasma bubbles imaged at geomagnetic conjugate points. In: Annales Geophysicae, vol. 22, pp. 31373143 (2004). Copernicus GmbH.

[36] Ma, G., Hocke, K., Li, J., Wan, Q., Lu, W., Fu, W.: Gnss ionosphere sounding of equatorial plasma bubbles. Atmosphere 10(11), 676 (2019). https://doi.org/10.3390/atmos10110676

[37] Kumar, S., Chen, W., Liu, Z., Ji, S.: E ects of solar and geomagnetic activity on the occurrence of equatorial plasma bubbles over hong kong. Journal of Geophysical Research: Space Physics 121(9), 91649178 (2016). https://doi.org/10.1002/2016JA02287315

[38] Basu, S., MacKenzie, E., Basu, S.: Ionospheric constraints on vhf/uhf communications links during solar maxi mumandminimumperiods. Radio Science 23(03), 363378 (1988). https://doi.org/10.1029/RS023i003p00363

[39] Abdu, M. A., Sobral, J. H. A., Batista, I. S., Rios, V., Medina, C.: Equatorial spread-f occurrence statistics in the american longitudes: Diurnal, seasonal and solar cycle variations. Advances in Space Research 22(6), 851854 (1998). https://doi.org/10.1016/S0273-1177(98)00111-2

[40] Basu, S., Groves, K., Basu, S., Sultan, P.: Speci cation and forecasting of scintillations in communication/navigation links: Current status and future plans. Journal of atmospheric and solar-terrestrial physics 64(16), 17451754 (2002). https://doi.org/10.1016/S1364-6826(02)00124-4

[41] Sobral, J. H. A., Abdu, M. A., Takahashi, H., Taylor, M. J., De Paula, E., Zamlutti, C. J., De Aquino, M., Borba, G.: Ionospheric plasma bubble climatology over brazil based on 22 years (19771998) of 630nm airglow observations. Journal of Atmospheric and Solar-Terrestrial Physics 64(12-14), 15171524 (2002). https://doi.org/10.1016/S1364-6826(02)00089-5

[42] Nishioka, M., Saito, A., Tsugawa, T.: Occurrence characteristics of plasma bubble derived from global ground based gps receiver networks. Journal of Geophysical Research: Space Physics 113(A5) (2008). https://doi.org/10.1029/2007JA012605

[43] Abiriga, F., Amabayo, E. B., Jurua, E., Cilliers, P. J.: Statistical characterization of equatorial plasma bubbles over east africa. Journal of Atmospheric and Solar-Terrestrial Physics 200, 105197 (2020). https://doi.org/10.1016/j.jastp.2020.105197

[44] Lee, C.-C., Liu, J.-Y., Reinisch, B., Chen, W.-S., Chu, F.-D.: The e ects of the pre-reversal exb drift, the eia asymmetry, and magnetic activity on the equatorial spread f during solar maximum. In: Annales Geophysi cae, vol. 23, pp. 745751 (2005). https://doi.org/10.5194/angeo-23-745-2005,2005. Copernicus Publications Gottingen, Germany.

[45] Manju, G.: On the seasonal varations of the threshold height for the occurrence of equatorial spread f during solar minimum and maximum years. Ann. Geophys. 25, 1 (2007) https://doi.org/10.5194/angeo-25-855-2007

Biography

Amsalu Hundessa Dinede, amse2022amse2014@gmail.com, Washera Geospace and Radar Science Research Laboratory, Bahir Dar, Ethiopia. Department of Physics and College of Science, Bonga University, Bonga, Ethiopia.